RSC Advances




ROYAL SOCIETY OF CHEMISTRY

www.rsc.org/advances

**TOC Figure**

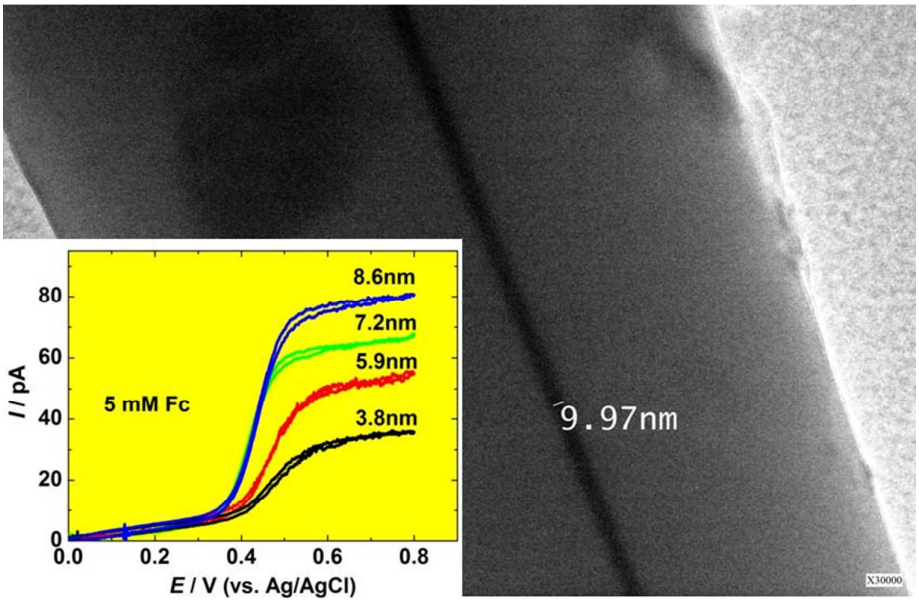


Single Au nano-disk nanoelectrodes with the radii down to 5 nm have been prepared, which can be used to measure ferritin molecules in the amount of ~3900 molecules or 6.1 zmol.

# Preparation, Electrochemical Responses and Sensing Application of Au Disk Nanoelectrodes Down to 5 nm

Yaoyao Zhang, Shen Xu, YuanYuan Qian, Xiaosong Yang, and Yongxin Li *

College of Chemistry and Materials Science, Anhui Normal University, Wuhu 241000, China

* Corresponding author. Ph, 86-553-3869302; Fax, 86-553-3869303

Email: yongli@mail.ahnu.edu.cn

**Abstract**

In this work, we report the preparation and electrochemical responses of Au disk nanoelectrodes as small as 5 nm in radii by the improvement of laser-assisted pulling technique. A Au microwire is sealed into a bilayer capillary and pulled into an ultrasharp Au nanowire sealed in a silica tip using a laser-assisted puller. The ultrasharp tip is then sealed into a piece of glass tube, which is manually polished to expose the Au. Transmission electron microscopy, steady-state voltammetry of small redox species (e.g., ferrocene (Fc), ferrocene methanol ($FcH_2OH$), potassium ferricyanide ($Fe(CN)_6^{3-}$), hexaammineruthenium(III) chloride ($Ru(NH_3)_6^{3+}$)), and cyclic voltammetry in a $H_2SO_4$ solution are utilized to characterize the nanoelectrodes. The heterogeneous electron transfer rate constant for the oxidation/reduction of Fc, $FcH_2OH$, $Fe(CN)_6^{3-}$, and $Ru(NH_3)_6^{3+}$ are determined from steady-state voltammetry using the method developed by Mirkin and Bard and found to be $k^o$ = 7.9 ± 3.6 cm/s and $\alpha$ = 0.41 ± 0.04 for Fc, $k^o$ = 7.4 ± 7.1 cm/s and $\alpha$ = 0.41 ± 0.23 for $FcCH_2OH$, $k^o$ = 4.0 ± 3.6 cm/s and $\alpha$ = 0.52 ± 0.17 for $Fe(CN)_6^{3-}$, and $k^o$ = 7.2 ± 6.9 cm/s and $\alpha$ = 0.53 ± 0.22 for $Ru(NH_3)_6^{3+}$. These Au disk nanoelectrodes have been used to investigate the direct electrochemistry of ferritin molecules, which are immobilized on Au surface by electrostatic interaction between the cysteamine monolayer modified on Au surface and ferritin molecules. From the voltammetric peak of ferritin on Au nanoelectrode (200 nm in radius), the amount of ~3900 molecules or 6.1 zmol can be calculated.

**Keywords:** nanoelectrodes, laser-assisted pulling technique, ferritin, gold

## 1. INTRODUCTION

Electrodes with nano-scale size have shown tremendous advantages such as smaller RC constants, faster mass-transport rates, and lower influences from solution resistance.[1-7] Due to their small size, nanoelectrodes are exhibiting their extensive applications in numerous areas, such as the study of electron transfer kinetics,[8-11] detection of single molecules and single nanoparticles,[12-14] high-resolution imaging in scanning electrochemical microscopy (SECM) and scanning tunneling microscopy (STM),[15-21] atomic force microscopy (AFM),[22] and chemical analysis and bioanalysis.[23-26]

In the past decades, several different methods have been reported producing single nanoelectrodes of submicrometer dimensions, which include glass encapsulation,[3, 27] electrochemical/chemical etching techniques followed by electrodeposition,[11, 28, 29] and micropipette/ capillary pulling and microfabrication,[16, 30] etc. Among above methods, the use of a laser puller for the fabrication of nanoelectrodes has its advantage such as simple, rapidness and good reproducibility.[5, 7, 10, 12, 18, 21, 24, 26, 29, 31, 32] Mirkin's group has reported the preparation and electrochemical responses of nanoelectrodes,[7, 10, 18, 21, 24, 26, 29, 31-33] and also investigated their applications in the adsorption/desorption of hydrogen,[33] electron transfer reactions,[10, 18, 34] and electrocatalysis,[35, 36] etc. Schuhmann's group and Sun's group have each discussed the fabrication process of Pt nanoelectrodes.[16, 17, 37] Zhang's group reported recently the preparation and characterization of the Pt nanoelectrode with a radius of 1-3 nm,[5] which can be used to fabricate single gold

nanoelectrode[12, 14] and single nanowire electrode.[38]

Most of nanoelectrodes previously fabricated in Zhang's group were made of Pt.[5, 12, 38] It is well-known that other metal (e.g., Au) electrodes have more extensively applications due to the good reaction activity of gold surface (e.g., surface modification through molecular self-assembly,[39] electrocatalysis,[40] bioanalysis[41]). Many attempts have been reported to address the fabrication of Au nanoelectrode using laser-assisted pulling technique.[27, 32, 42] Mirkin et al. recently developed gold nanotips to study the electron transfer rate using SECM.[32] Zhang's group and Shi's group also fabricated gold disk nanoelectrodes.[42, 43] Because the melting point of gold (1064 °C) is lower than platinum (1710 °C), it is still a challenge to fabricate single Au nanoelectrodes within extremely small size (e.g., $r$ < 5 nm), and this would limit their applications such as bio-analysis and catalysis.

In this paper, we wish to focus on the fabrication and characterization of Au disk electrodes scaling down to 5 nm in radii. **Figure 1** shows transmission electron microscopy (TEM) image of a 5 nm radius Au nanowire sealed in $SiO_2$. These electrodes were fabricated by a laser-assisted pulling process with several key modifications in our laboratory, which include bilayer capillary and epoxy sealing after pulling. An electrical continuity tester is used to monitor the polishing process. The Au nanoelectrodes fabricated in this study have been utilized to measure the standard heterogeneous electron transfer (ET) rate constant, $k^o$, for several redox species, including ferrocene (Fc), ferrocene methanol ($FcH_2OH$), potassium ferricyanide ($Fe(CN)_6^{3-}$), hexaammineruthenium(III) chloride ($Ru(NH_3)_6^{3+}$, in acetonitrile or

aqueous solution. It has been found that the obtained values of $k^o$ in this method are similar to previous results reported by our and other groups.[8, 18, 44-46] This Au nanoelectrode has also been used to investigate the direct electrochemistry of ferritin molecules and the amount of ~3900 molecules or 6.1 zmol can be calculated from the voltammetric peak of ferritin on Au nanoelectrode (200 nm in radius).

## 2. EXPERIMENTAL SECTION

**Chemicals.** Ferrocene (Fc, Fluka), ferrocene methanol ($FcCH_2OH$, Aldrich), hexaammineruthenium(III) chloride ($Ru(NH_3)_6Cl_3$; Aldrich), Potassium ferricyanide ($K_3Fe(CN)_6$; Acros Organics), tetra-*n*-butylammonium hexafluorophosphate ($TBAPF_6$, Aldrich), potassium chloride (KCl, Shanghai Chemical Company, Shanghai, China), and acetonitrile (ACN, Shanghai Chemical Company, Shanghai, China), ferritin (from equine spleen, Sigma), cysteamine hydrochloride (Fluka) were of reagent grade quality or better and used without further purification. Aqueous and organic solutions were prepared from deionized water (Milli-Q, Millipore Co.) and acetontrile, respectively.

Au microwires with a diameter of 25 $\mu$m (99.95%, hard) were purchased from Alfa Aesar. Borosilicate glass capillaries (*o.d.* = 1.0 mm; *i.d.* = 0.64 mm) were obtained from Sutter Instrument Co. A silverfilled epoxy glue (DuPont) was used to contact the Au wire with a tungsten wire. Alumina polishing powders with different particle sizes of 1.0, 0.3, and 0.05 $\mu$m and fine grit sandpapers with 400, 600, and 800 grits were purchased from Buehler.

**Transmission Electron Microscopy.** TEM images of $SiO_2$-coated Au nanoelectrodes were acquired on a Tecnai G2 F20 (FEI) microscope. No additional coatings were performed prior to imaging.

**Nanoelectrode Preparation.** The Au disk nanoelectrodes were prepared utilizing a four-step process, which is similar to the fabrication process of Pt with some changes.[5, 32] The details of the fabrication procedure were provided in *supporting information.* Briefly, a 25 *μ*m Au wire was sealed into a 1-cm long piece of a silica capillary with an inner diameter of ~ 80 *μ*m and an outer diameter of ~ 300 *μ*m with the help of a stereo microscope. The small silica capillary/Au ensemble was then inserted into the center of a 7.5 cm long piece of a borosilicate glass capillary (*o.d.* = 1.0 mm; *i.d.* = 0.64 mm). The Au/bi-layer capillary assembly was sealed and then pulled into two ultra-sharp tips. The ultra-sharp was sealed with care into borosilicate glass tubing using epoxy, which was then polished with sandpaper to expose the Au nanodisk under the control of a homemade ultrasensitive continuity tester to ensure the polishing stops when the very end of Au is exposed.[47, 48] After that, the electrode was polished slightly by alumina polishing powders on a special cloth to make sure the surface is mirror-like.

**Ferritin immobilized on Au surface.** The Au nanoelectrode was modified with cysteamine by being immersed in an aqueous solution of cysteamine hydrochloride (10 mM) for 2 hour, and then washed by water.[49] The cysteamine monolayer will electrostatically capture ferritin molecules (pI = 4 ~ 5)[50] and also enhance the direct

electron transfer reaction of ferritin.[51, 52] Au disk microelectrode modified with cysteamine was prepared in the same manner for control experiment.

**Electrochemical measurements** Electrochemical measurements were carried out using a computer-controlled potentiostat (Dagan Chem-Clamp Voltammeter-Amperometer) and a biopotentostat connected to a scanning electrochemical microscope (SECM, 900B mode, CH Instrument). A one-compartment, two-electrode cell was employed with the cell and preamplifier in a home-built Faraday cage. A Ag/AgCl electrode (Bioanalytical Sciences, Inc.) was used as the reference electrode. All electrochemical experiments were performed at room temperature (25 °C).

## 3. RESULTS AND DISCUSSION

### 3.1. TEM image of Au Nanoelectrode.

TEM is one of most popular methods to provide atomic resolution structural information of nanomaterials. **Figure 1** shows the TEM image of a Au nanowire tip prepared from a 25 μm microwire perform. The Au nanowire with the radius of ~5 nm can be observed clearly, and the $SiO_2$−Au wire surface of the electrode is smooth and no obvious gap can be found. One more TEM image with the radius of ~ 18 nm is also provided in Supporting Information (**Fig. S1**). From the energy dispersive X-ray spectroscopy (EDX) result (shown in **Fig. S2**), it could be obtained that Au nanoelectrode was fabricated successfully.

### 3.2. Key improvements of the fabrication procedure to obtain Au

**nanoelectrodes down to 5 nm.**

The details of the fabrication of Au nanoelectrodes were provided in experimental section and supporting information. Because the melting point of gold (1064.18 °C) is lower than platinum (1773 °C), which makes it much difficult to pull the continuous Au ultra-sharp tips and nanoelectrodes. We have made the several revisions to get the Au nanoelectrodes within 5 nm. First, Au microwire was inserted to a small silica capillary with an inner diameter of ~ 80 $\mu$m, which can improve the stability of the following sealing and pulling steps.[5] Second, the programs designed to pull Au/bi-layer capillary assemby were changed compared to pull Pt/capillary assembly. For example, the parameter heat that control the output power of a laser was set lower for gold (560) than for platinum (820),[5] but the parameter velocity was higher for gold (100) than for platinum (80). Third, it is necessary to seal the Au ultra-sharp tips into glass tube. Most of the nanoelectrodes were polished using a special beveler to expose the Pt/Au wire.[16, 18, 53] However, extremely small size of the Au tip makes it hard to expose the Au by direct polishing on a surface without breaking the tip and it is hard to get the exposed Au tip within 10 nm. In our experiment, we sealed the Au ultra-sharp tip into a 2 mm borosilcate glass tube with epoxy. Finally, the sealed Au ultra-sharp tips were directly polished on fine sandpapers and aluminum oxide powers under the control of a homemade ultrasensitive continuity tester to ensure the polishing stops when the very end of Au is exposed.[47, 48]

With above improvement, the fabrication process can be well-controlled, which resulting in > 90% reproducibility in obtaining Au electrodes < 5 nm in radii.

### 3.3. Voltammetric Responses of Au Nanoelectrodes.

**Figure 2** shows the voltammetric responses of Au nanoelectrodes with different sizes in an ACN solution containing 5 mM Fc and 0.2 M TBAPF6 (A), a 1 mM $FcCH_2OH$ containing 0.1 M KCl (B), a 5 mM $K_3Fe(CN)_6$ containing 0.2 M KCl (C), and a 5 mM $Ru(NH_3)_6Cl_3$ containing 0.2 M KCl (D). Assuming a disk-shaped geometry of the Au nanoelectrode embedded in an infinite large insulation material, the radius of the electrode can be calculated from the diffusion-limited steady-state current:[54]

$$i_d = 4nFDC_ba \quad (1)$$

where n is the number of electrons transferred per molecule, $F$ is Faraday's constant, $D$ and $C_b$ are the diffusion coefficient and bulk concentration of the redox molecule, respectively. The radius of the nanodisk electrode, $a$, is determined by measuring $i_d$ for the oxidation Fc, $FcCH_2OH$, $Fe(CN)_6^{3-}$ or $Ru(NH_3)_6^{3+}$. In agreement with theory and previous results of voltammetric response at nanodisk electrodes,[30] all the voltammograms have an ideal sigmoidal shape and display no obvious hysteresis on the reverse scan, and the curve deviations are relatively small due to ohmic resistance or overlaying capacitance, even for the smallest electrodes with radii down to 3.8 nm, as shown in **Figure 2(A)**, which is much smaller than the previous result prepared by laser-assisted pulling process.[32, 42] The EC diffusion process was simulated by COMSOL[47, 48] using 5 mM Fc ACN solution and 5-nm Au disk electrode in radius **(Figure S3**). The calculated current value from COMSOL simulation is almost the same obtained from the CV experimental result **(Figure S4, Figure S5)**,

indicating the prepared Au nanoelectrode is well-sealed and has good EC response. However, Amemiya et al. recently found that damaged Pt nanoelectrodes could show perfect voltammetric responses.[55] To investigate the surface property of Au nanodisc electrode, the voltammograms with different scan rates have been collected (**Figure S6**). From **Figure S6**, it can be seen that both the curves are retraceable and well-shaped, with a flat plateau and negligibly small background current. Although the capacitive contribution is more significant at higher scan rate (2.0 V/s, red curve in **Figure S6**), the overall shape of both votammograms is steady-state, indicating no solution-filled cavity existed at the surface of the nanodisc surface.

**3.4. Cyclic Votammetry of Au Nanoelectrodes in $H_2SO_4$.** The cyclic voltammetry (CV) in $H_2SO_4$ solution is often used as a finger-print method for the characterization of different metal electrodes, especially for Pt and Au electrodes based on their characteristic voltammograms for the formation of surface oxides and their subsequent reduction processes in acid electrolytes.[12, 42] After successful fabrication of Au disk nanoelectrodes, the cyclic voltammograms using Au nanoelectrodes with different radii were recorded in 0.5 M $H_2SO_4$ solution, and the results were provided in **Figure 3**. **Figure 3** shows the cyclic voltammograms of three Au nanoelectrodes with a radius of (a) 12.2 nm, (b) 28.6 nm, and (c) 32.3 nm, at a scan rate of 50 mV/s. As it can be found, all of the Au nanoelectrodes show typically characteristic voltmmograms: during the forward sweep, the current increases at ~ 1.2 V vs. Ag/AgCl corresponding to the formation of Au surface oxide; during the backward

sweep, a reduction peak appears at ~ 0.95 V vs. Ag/AgCl corresponding to the reduction of Au oxide. Interestingly it can be observed that the peak potential of the reduction peak has a slightly shift towards negative direction for smaller Au nanoelectrodes, which was also reported by Zhang et al.[42] and Zamborini et al.[55] This size-dependent potential shift may be due to a change in the standard redox potential of Au and Au oxide.

**3.5. Electron-Transfer Rate Constant Measured at Au Nanoelectrodes.** It is well-known that the measurement of $k^o$ requires that the rate of mass transfer of the molecule to the electrode surface be comparable to or greater than the rate of electron transfer.[8] For steady-state voltammetry at a hemispherical or disk electrode involving purely diffusional transport, this condition can be expressed as[56, 57]

$$(D/k^o a) \geq 0.1 \quad (2)$$

Generally, values of $k^o$ between 1 and 100 cm/s can be measured using electrodes with a between 100 and 1 nm, assuming a typical value of $D$ (~$10^{-5}$ $cm^2$/s). Therefore, it is appropriate to measure the ET rate constants for the oxidation of Fc, $FcCH_2OH$, $Fe(CN)_6^{3-}$, and $Ru(NH3)_6^{3+}$ using the Au nanoelectrodes prepared in this work.

Herein, steady-state voltammetric responses of Au nanoelectrodes were employed to measure the standard heterogeneous ET rate constant, $k^o$, for Fc, $FcCH_2OH$, $Fe(CN)_6^{3-}$, and $Ru(NH3)_6^{3+}$, respectively. The voltammetric responses of Au nanoelectrodes are shown in **Figure 4A**, **Figure 4B**, **Figure 4C** and **Figure 4D** for Fc, $FcCH_2OH$, $Fe(CN)_6^{3-}$, and $Ru(NH3)_6^{3+}$, respectively. Then the voltammetric current

of each redox species is normalized to its diffusion-controlled limiting current based on the oxidation wave, $i_d$, to better display the relationship between voltammetric response and the radius of the nanoelectrode, and the normalized currents are shown in **Figure S7A**, **Figure S7B**, **Figure S7C** and **Figure S7D**. From the normalized voltammograms of each redox species with different radii shown in **Figure S7**, it can be easily obtained that the voltammetric half-wave potential, $E_{1/2}$, shifts towards more positive potentials as the decreases of radii, which is similar to previous results.[8]

Assuming the voltammetric results shown in **Figure 4** and **Figure S7** are fit to classical Butler-Volmer electrode kinetics, the *i-E* relationship for the oxidation of Fc, $FcCH_2OH$, $Fe(CN)_6^{3-}$, and $Ru(NH_3)_6^{3+}$ can be written as[56]

$$i = \frac{nFAC^{*}k^{o}\exp((1-\alpha)F(E-E^{o\prime})/RT)}{1+\frac{ak^{o}}{D}[\exp(-\alpha F(E-E^{o\prime})/RT)+\exp((1-\alpha)F(E-E^{o\prime})/RT)]} \quad (3)$$

where $A$ is known generally as the frequency factor, $E^{o\prime}$ is formal potential of an electrode, $\alpha$ is the transfer coefficient, $T$ is absolute temperature, and other parameters have been previously defined. According to the method developed by Mirkin and Bard,[58] the values of $k^o$ and $\alpha$ can be calculated based on the measurement of experimental parameters ($E_{1/4} - E_{1/2}$) and ($E_{1/2} - E_{3/4}$) in **Figure 4** and **Figure S7**, where $E_{1/4}$ and $E_{3/4}$ are the quartile potentials, corresponding to the electrode potentials where the current is equal to 1/4 and 3/4 of the limiting value, respectively. Values of $k^o$ and $\alpha$ for the oxidation of Fc, $FcCH_2OH$, $Fe(CN)_6^{3-}$, and

$Ru(NH_3)_6^{3+}$, determined by this method for different size nanoelectrodes, with radii ranging from 0.6 to 183.6 nm, are listed in **Table S1**, **Table S2**, **Table S3** and **Table S4**, respectively. So the average values of $k^o$ and $\alpha$ for the oxidation of Fc, $FcCH_2OH$, $Fe(CN)_6^{3-}$, and $Ru(NH_3)_6^{3+}$ can be obtained as $k^o$ = 7.9 ± 3.6 cm/s and $\alpha$ = 0.41 ± 0.04 for Fc, $k^o$ = 7.4 ± 7.1 cm/s and $\alpha$ = 0.41 ± 0.23 for $FcCH_2OH$, $k^o$ = 4.0 ± 3.6 cm/s and $\alpha$ = 0.52 ± 0.17 for $Fe(CN)_6^{3-}$, and $k^o$ = 7.2 ± 6.9 cm/s and $\alpha$ = 0.53 ± 0.22 for $Ru(NH_3)_6^{3+}$, respectively. Our measured results for $k^o$ and $\alpha$ are reasonable as compared to values previously reported by other groups.[8, 44-46] However, it must be pointed out that the mean rate constant value at Au surface ($k^o$ = 7.2 ± 6.9 cm/s) in this work is lower than that measured at Au tips using SECM method ($k^o$ = 13.5 ± 2.0 cm/s),[32] which is different from the results of Iwasita et al.[59] We think it may be due to the different supporting electrolyte because the kinetics of $Ru(NH_3)_6^{3+}$ reduction strongly depends on the nature of the supporting electrolyte, and the $k^o$ value greatly increases in a high concentration of chloride. Finally it should be pointed out that the method developed by Mirkin and Bard [58] is only used to the condition that the experimental voltammograms is fit the theoretical value exactly. Unfortunately it is hard to get these accurate values because the experimental conditions are always affected by different issues such as temperature, ion strength, concentration, etc. The values of the parameters calculated here are just used to estimate the ET constants got from the nanoelectrodes with different radii.

**3.6. CVs of Ferritin Adsorbed on Au Nanoelectrode.** It is well-known that Au elecrode is one of the easiest surfaces to be modified due to the strong Au-S bond and can be used to investigate the redox response of very few molecules.[42] Watkins et al. have carefully investigated the redox response of bis(2,2'-bipyridine)chloro(4,4'-trimethylenedipyridine)osmium(II) molecules adsorbed on a Pt nanoelectrode.[8] Zhang et al.[42] and Hoeben et al.[25] have reported the redox responses of $2.3 \times 10^6$ ferrocene molecules and less than 50 [NiFe]-Hydrogenase Proteins on Au nanoelectrodes, respectively. Herein ferritin molecules were immobilized on the surface of Au nanoelectrodes and their redox responses were investigated. **Figure 5a** shows CVs of Au nanoelectrode after immersion in 5 mg/mL ferritin solution for 2 hours. It can be a cathodic peak ~ - 0.34 V and an anodic peak ~ - 0.19 V were observed in the first cycle, which were originated from the direct electron transfer reaction of ferritin immobilized on the Au surface.[51, 60-63] In the subsequent cycles, the cathodic peak shifted to more positive potential (- 0.30 V), probably reflecting the reconstruction of the ferritin layer on Au surface, which was reported previously when ferritin adsorbed onto tin-doped indium oxide electrodes and nanopore recessed Au electrode.[52, 61] Moreover, the cathodic current gradually decreased probably due to the release of Fe(II) from the ferritin molecules.[51, 52, 61, 62] A similar shift in cathodic potential and a gradual decrease in the charge were observed on cysteamine-modified gold substrates with micro-size (25 μm, **Figure 5b**). The number of ferritin molecules adsorbed on the Au surface can be calculated based on the following equation[8, 42]

$$\Gamma^* = Q/nFA \quad (4)$$

Where $\Gamma^*$ is the surface coverage of ferritin, Q is the charge associated with the voltammetric peak, *n* is the number of electrons transferred per redox molecules (*n* is ~ 4500 for ferritin[52, 64]), *F* is the Faraday's constant, and *A* is the area of the Au electrode, respectively. The total number of the electrons transferred has been integrated to be $2.8 \times 10^{-12}$ C, which corresponds to ~ 3900 molecules or ~ 6.1 zmol. Assuming the planar cysteamine-modified gold surface was completely covered with ferritin upon (i.e., 8 x $10^3$ molecules/$\mu m^2$),[51, 52] the radius of the Au nanoelectrode can be calculated to be 393 nm, which is much bigger than the value calculated from eq *1* by small redox species. Considering the similar radii of Au microelectrode calculated from eq *4* and eq *1* (14.8 μm calculated from eq *4 vs.* 12.5 μm calculated from eq *1*), it can be obtained that the surface roughness factor of Au nanoelectrode (~ 1.96) is much bigger than that from Au micro/macro electrodes (~1.18).

Based on the relationship between peak voltmammetric current and the scan rate given as follows,[57] it can be obtained that increasing scan rate will be helpful to get large peak current. Because this result was obtained at a slow scan rate (100 mV/s) on a relatively large Au nanaoelectrode (radius: 200 nm), we believe that more improvement can be investigated to get the voltammetric response from much less redox molecules.

$$i_p = (n^2F^2/4RT)vA\Gamma^* \quad (5)$$

## 4. CONCLUSIONS

Au disk nanoelectrodes with the radii down to 5 nm have been prepared through improved laser-assisted pulling technique, which have been characterized by TEM and voltammetry in small redox species and $H_2SO_4$ solution. These Au disk nanoelectrodes have been employed to measure the rapid heterogeneous ET rate constant of four different redox species, and the results are in good agreement with the values reported previously. From the voltammetric peak of ferritin on Au nanoelectrode (200 nm in radius), the amount of ~3900 molecules or 6.1 zmol can be calculated. The results from the direct electrochemistry of ferritin immobilized on Au disk nanoelectrodes demonstrate the ability of electrode at nanoscale to detect zeptomole quantities of an electroactive species, indicating that the Au disk nanoelectrodes can be applied in many interesting studies, such as single molecule/nanoparticle detection, bioanalysis, electrocatalytic effects of novel materials at the nanoscale.

**Acknowledgments.** We thank Prof. Bo Zhang (University of Washington) for his useful suggestion and discussion. This work is financially supported by the National Natural Science Foundation of China (No.20975002), the Key Project of Chinese Ministry of Education (No. 212083) and Anhui Normal University.

## SUPPORTING INFORMATION AVALALBLE

Electronic supplementary information (ESI) available. See DOI: 10.103/xxxx

## REFERENCES

1. R. W. Murray, *Chemical Reviews*, 2008, **108**, 2688-2720.
2. J. Abbou, C. Demaille, M. Druet and J. Moiroux, *Analytical Chemistry*, 2002, **74**, 6355-6363.
3. R. M. Penner, M. J. Heben, T. L. Longin and N. S. Lewis, *Science*, 1990, **250**, 1118-1121.
4. J. T. Cox and B. Zhang, *Annual Review of Analytical Chemistry, Vol 5*, 2012, **5**, 253-272.
5. Y. X. Li, D. Bergman and B. Zhang, *Analytical Chemistry*, 2009, **81**, 5496-5502.
6. D. W. M. Arrigan, *Analyst*, 2004, **129**, 1157-1165.
7. J. Velmurugan, J. M. Noel and M. V. Mirkin, *Chem. Sci.*, 2014, **5**, 189-194.
8. J. J. Watkins, J. Y. Chen, H. S. White, H. D. Abruna, E. Maisonhaute and C. Amatore, *Analytical Chemistry*, 2003, **75**, 3962-3971.
9. B. Zhang, L. X. Fan, H. W. Zhong, Y. W. Liu and S. L. Chen, *Journal of the American Chemical Society*, 2013, **135**, 10073-10080.
10. P. Sun, Z. Liu, H. Yu and M. V. Mirkin, *Langmuir*, 2008, **24**, 9941-9944.
11. P. Sun, Z. Q. Zhang, J. D. Guo and Y. H. Shao, *Analytical Chemistry*, 2001, **73**, 5346-5351.
12. Y. X. Li, J. T. Cox and B. Zhang, *Journal of the American Chemical Society*, 2010, **132**, 3047-3054.
13. J. Lakbub, A. Pouliwe, A. Kamasah, C. Yang and P. Sun, *Electroanalysis*, 2011, **23**, 2270-2274.
14. P. Sun, F. Li, C. Yang, T. Sun, I. Kady, B. Hunt and J. Zhuang, *J. Phys. Chem. C*, 2013, **117**, 6120-6125.
15. M. V. Mirkin, W. Nogala, J. Velmurugan and Y. X. Wang, *Physical Chemistry Chemical Physics*, 2011, **13**, 21196-21212.
16. B. B. Katemann and T. Schuhmann, *Electroanalysis*, 2002, **14**, 22-28.
17. B. B. Katemann, A. Schulte and W. Schuhmann, *Electroanalysis*, 2004, **16**, 60-65.
18. P. Sun and M. V. Mirkin, *Analytical Chemistry*, 2006, **78**, 6526-6534.
19. M. Etienne, E. C. Anderson, S. R. Evans, W. Schuhmann and I. Fritsch, *Analytical Chemistry*, 2006, **78**, 7317-7324.
20. M. V. Mirkin, L. O. S. Bulhoes and A. J. Bard, *Journal of the American Chemical Society*, 1993, **115**, 201-204.
21. Y. Wang, K. Kececi, J. Velmurugan and M. V. Mirkin, *Chemical Science*, 2013, **4**, 3606-3616.
22. W. Nogala, J. Velmurugan and M. V. Mirkin, *Analytical Chemistry*, 2012, **84**, 5192-5197.
23. A. G. Ewing, D. Omiatek, L. Mellander, Y. Dong, M. Heien and B. Zhang, *Abstracts of Papers of the American Chemical Society*, 2011, **241**.
24. Y. X. Wang, J. M. Noel, J. Velmurugan, W. Nogala, M. V. Mirkin, C. Lu, M. G. Collignon, F. Lemaitre and C. Amatore, *Proc. Natl. Acad. Sci. U. S. A.*, 2012, **109**, 11534-11539.
25. F. J. M. Hoeben, F. S. Meijer, C. Dekker, S. P. J. Albracht, H. A. Heering and S. G. Lemay, *Acs Nano*, 2008, **2**, 2497-2504.
26. P. Sun, F. O. Laforge, T. P. Abeyweera, S. A. Rotenberg, J. Carpino and M. V.

Mirkin, *Proceedings of the National Academy of Sciences of the United States of America*, 2008, **105**, 443-448.
27. B. Zhang, J. Galusha, P. G. Shiozawa, G. Wang, A. J. Bergren, R. M. Jones, R. J. White, E. N. Ervin, C. C. Cauley and H. S. White, *Analytical Chemistry*, 2007, **79**, 4778-4787.
28. J. Velmurugan, J.-M. Noel and M. V. Mirkin, *Chemical Science*, 2014, **5**, 189-194.
29. J. Velmurugan, J.-M. Noel, W. Nogala and M. V. Mirkin, *Chemical Science*, 2012, **3**, 3307-3314.
30. Y. H. Shao, M. V. Mirkin, G. Fish, S. Kokotov, D. Palanker and A. Lewis, *Analytical Chemistry*, 1997, **69**, 1627-1634.
31. J. Velmurugan and M. V. Mirkin, *Chemphyschem*, 2010, **11**, 3011-3017.
32. J. Velmurugan, P. Sun and M. V. Mirkin, *J. Phys. Chem. C*, 2009, **113**, 459-464.
33. D. Zhan, J. Velmurugan and M. V. Mirkin, *Journal of the American Chemical Society*, 2009, **131**, 14756-14760.
34. Y. X. Wang, K. Kececi, J. Velmurugan and M. V. Mirkin, *Chem. Sci.*, 2013, **4**, 3606-3616.
35. J.-M. Noel, Y. Yu and M. V. Mirkin, *Langmuir*, 2013, **29**, 1346-1350.
36. Y. Wang, J.-M. Noel, J. Velmurugan, W. Nogala, M. V. Mirkin, C. Lu, M. G. Collignon, F. Lemaitre and C. Amatore, *Proceedings of the National Academy of Sciences of the United States of America*, 2012, **109**, 11534-11539.
37. C. Yang and P. Sun, *Analytical Chemistry*, 2009, **81**, 7496-7500.
38. Y. X. Li, Q. Q. Wu, S. F. Jiao, C. D. Xu and L. Wang, *Analytical Chemistry*, 2013, **85**, 4135-4140.
39. H. Lin, H. Cheng, L. Liu, Z. Zhu, Y. Shao, P. Papakonstantinou, D. Mihailovic and M. Li, *Biosens. Bioelectron.*, 2011, **26**, 1866-1870.
40. T. d. F. Paulo, I. C. N. Diogenes and H. D. Abruna, *Langmuir*, 2011, **27**, 2052-2057.
41. K. Dawson, A. Wahl, R. Murphy and A. O'Riordan, *J. Phys. Chem. C*, 2012, **116**, 14665-14673.
42. B. K. Jena, S. J. Percival and B. Zhang, *Analytical Chemistry*, 2010, **82**, 6737-6743.
43. Y. Liu, M. Li, F. Zhang, A. Zhu and G. Shi, *Analytical Chemistry*, 2015, **87**, 5531 - 5538.
44. D. O. K. Wipf, E. W.; Deakin, M. R.; Wightman, R. M., *Anal. Chem.*, 1988, **60**, 306-310.
45. J. J. Watkins and H. S. White, *Langmuir*, 2004, **20**, 5474-5483.
46. M. V. Mirkin, T. C. Richards and A. J. Bard, *J. Phys. Chem.*, 1993, **97**, 7672-7677.
47. B. Zhang, Y. Zhang and H. S. White, *Anal. Chem.*, 2004, **76**, 6229.
48. B. Zhang, Y. Zhang and H. S. White, *Anal. Chem.*, 2006, **78**, 477.
49. C. R. Raj and T. Ohsaka, *Electroanalysis*, 2002, **14**, 679-684.
50. E. C. Thiel, *Annu. Rev. Biochem.*, 1987, **56**, 289-315.
51. M. Tominaga, A. Ohira, Y. Yamaguchi and M. Kunitake, *J. Electroanal. Chem.*, 2004, **566**, 323-329.
52. Y. X. Li and T. Ito, *Analytical Chemistry*, 2009, **81**, 851-855.
53. S. E. Salamifar and R. Y. Lai, *Analytical Chemistry*, 2014, **86**, 2849-2852.
54. Y. Saito, *Rev. Polarogr.*, 1968, **15**, 177-187.

55. O. S. Ivanova and F. P. Zamborini, *Journal of the American Chemical Society*, 2010, **132**, 70-+.
56. C. G. Zoski, *In Modern Techniques in Electroanalysis*, Wiley, New York, 1996.
57. A. J. Bard and L. R. Faulkner, *Electrochemical Mthods.*, 2nd ed. edn., John Wiley & Sons, New York, 2001.
58. M. V. Mirkin and A. J. Bard, *Anal. Chem.*, 1992, **64**, 2293-2303.
59. T. Iwasita, W. Schmickler and J. W. Schultze, *Berichte Der Bunsen-Gesellschaft-Physical Chemistry Chemical Physics*, 1985, **89**, 138-142.
60. T. D. Martin, S. A. Monheit, R. J. Niichel, S. C. Peterson, C. H. Campbell and D. C. Zapien, *J. Electroanal. Chem.*, 1997, **420**, 279-290.
61. R. J. Cherry, A. J. Bjornsen and D. C. Zapien, *Langmuir*, 1998, **14**, 1971-1973.
62. M.-S. Pyon, R. J. Cherry, A. J. Bjornsen and D. C. Zapien, *Langmuir*, 1999, **15**, 7040-7046.
63. D. C. Zapien and M. A. Johnson, *J. Electroanal. Chem.*, 2000, **494**, 114-120.
64. A. Mohammadi, A. B. Moghaddam and J. Badraghi, *Analytical Methods*, 2012, **4**, 1024-1028.

**Figure Captions**

**Figure 1.** TEM image of single Au nanoelectrode sealed in $SiO_2$.

**Figure 2.** Voltammetric responses of Au nanoelectrodes in a 5 mM Fc ACN solution containing 0.2 M $TBAPF_6$ (A), 1 mM $FcCH_2OH$ containing 0.1 M KCl (B), 5 mM $K_3Fe(CN)_6$ containing 0.2 M KCl (C), and 5 mM $Ru(NH_3)_6Cl_3$ containing 0.2 M KCl (D). Scan rate is 10 mV/s.

**Figure 3.**The cyclic voltammograms in 0.5 M $H_2SO_4$ of three Au nanoelectrodes with the radii of (a) 12.2 nm, (b) 28.6 nm, and (c) 32.3 nm. Scan rate: 50 mV/s.

**Figure 4.** Voltammetric responses of Au nanoelectrodes in a 5 mM Fc ACN solution containing 0.1 M $TBAPF_6$ (A), 1 mM $FcCH_2OH$ containing 0.1 M KCl (B), 5 mM $K_3Fe(CN)_6$ containing 0.2 M KCl (C), and 5 mM $Ru(NH_3)_6Cl_3$ containing 0.2 M KCl (D). Scan rate is 10 mV/s.

**Figure 5.** Multiple potential cycles for ferritin immobilized on a gold nanoelectrode with a radius of 200 nm (a) and a gold microelectrode with a radius of 12.5 μm (b). CVs (scan rate, 100 mV/s) were measured in a 0.1 M $KH_2PO4$-$K_2HPO_4$ buffer at pH 7.0. The gold electrodes were modified with cysteamine by immersion in an aqueous solution of cysteamine hydrochloride (10 mM) for 2 h, followed by rinsing with water.

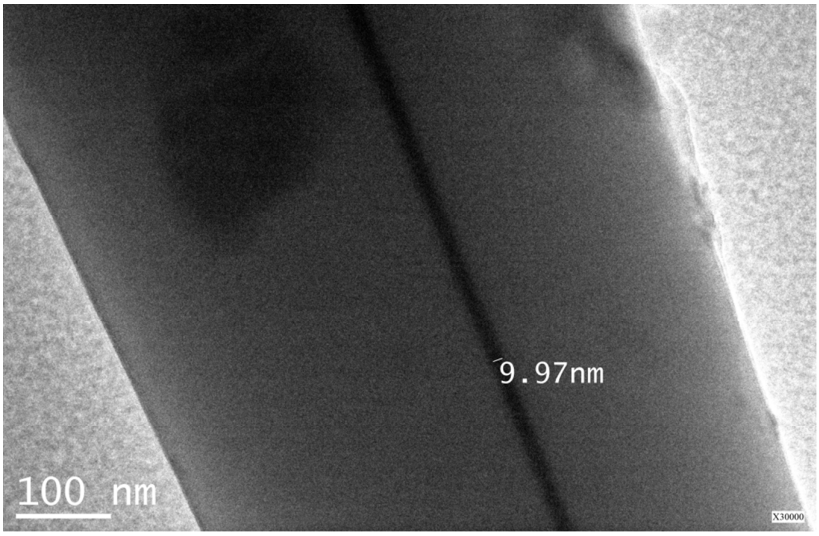


**Figure 1.**

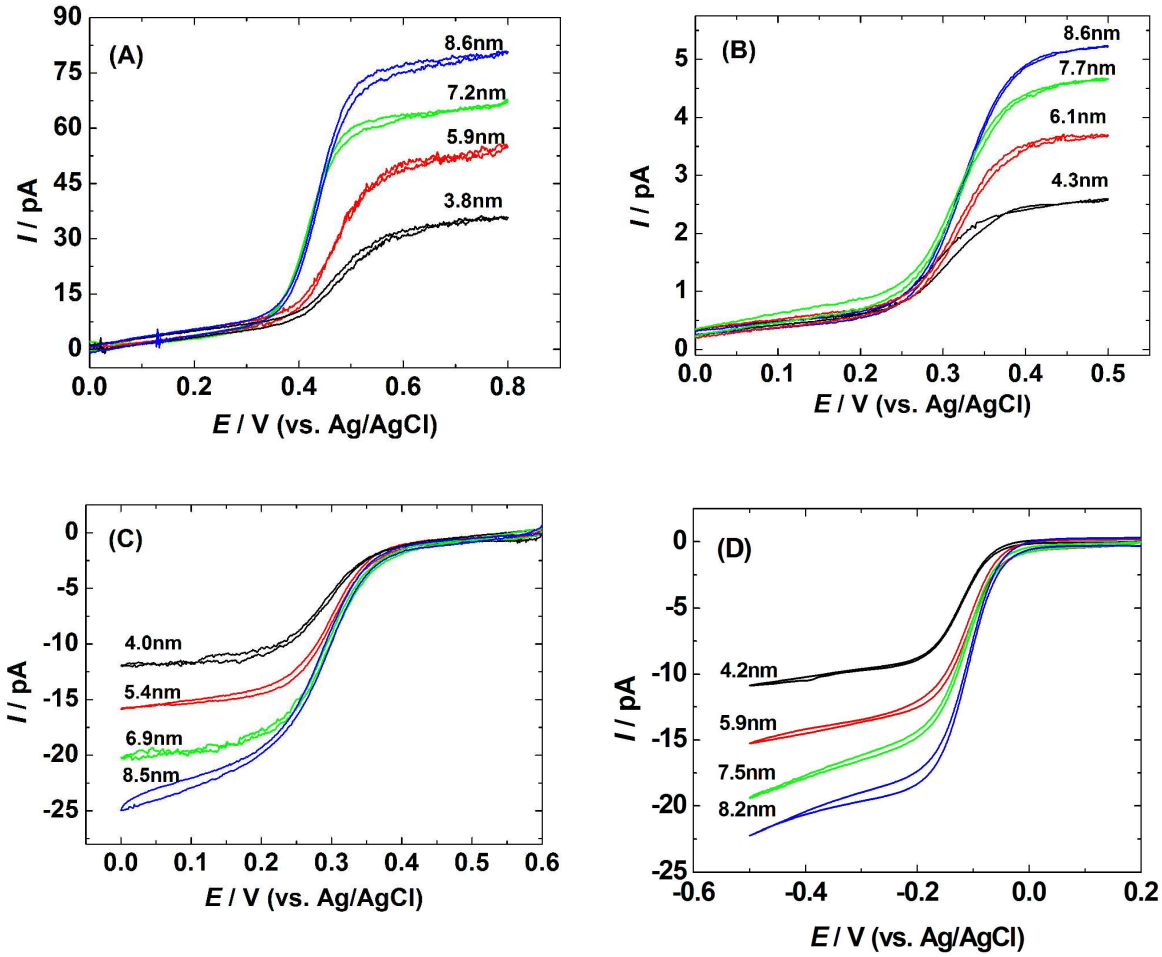


**Figure 2.**

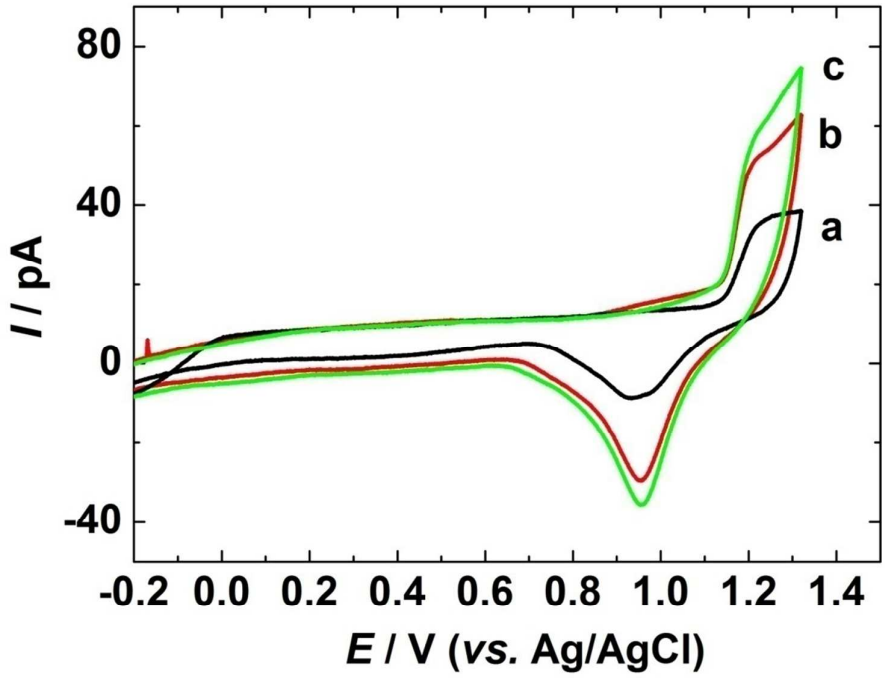


**Figure 3.**

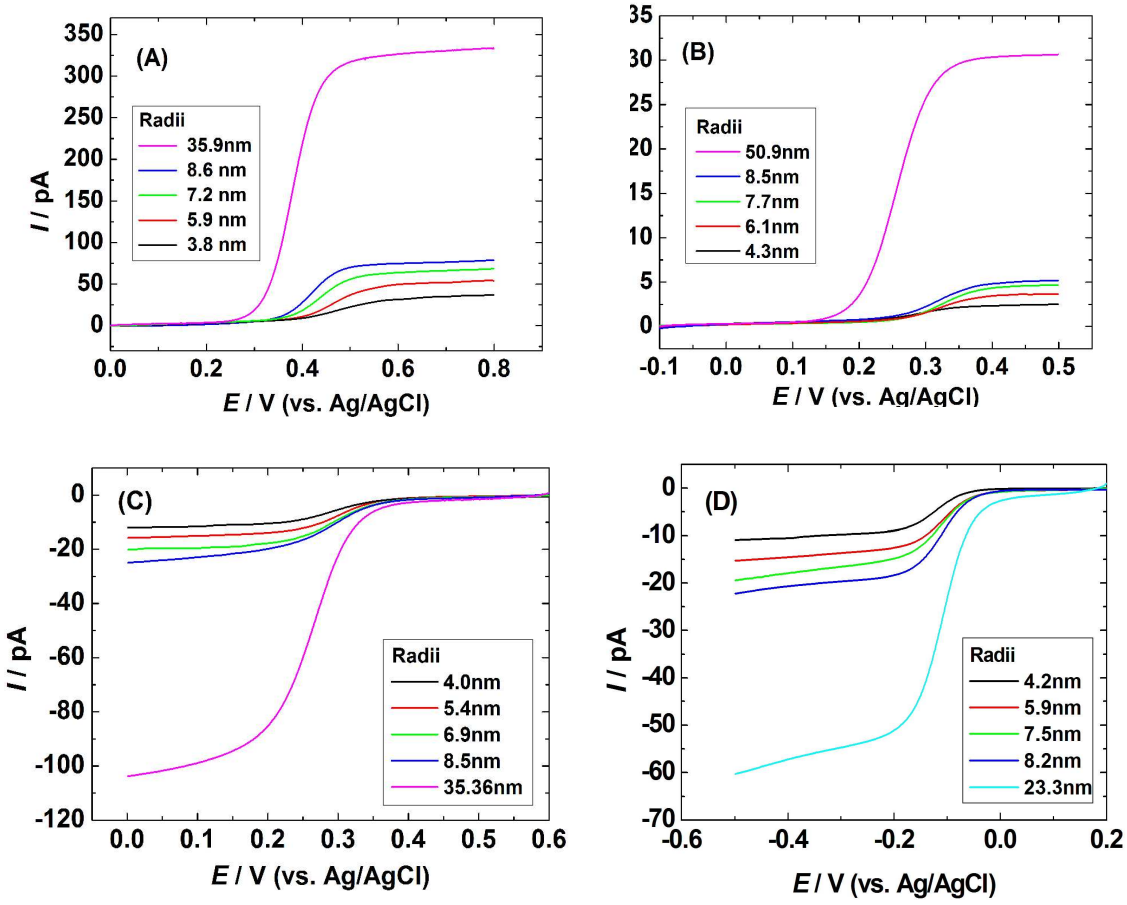


**Figure 4.**

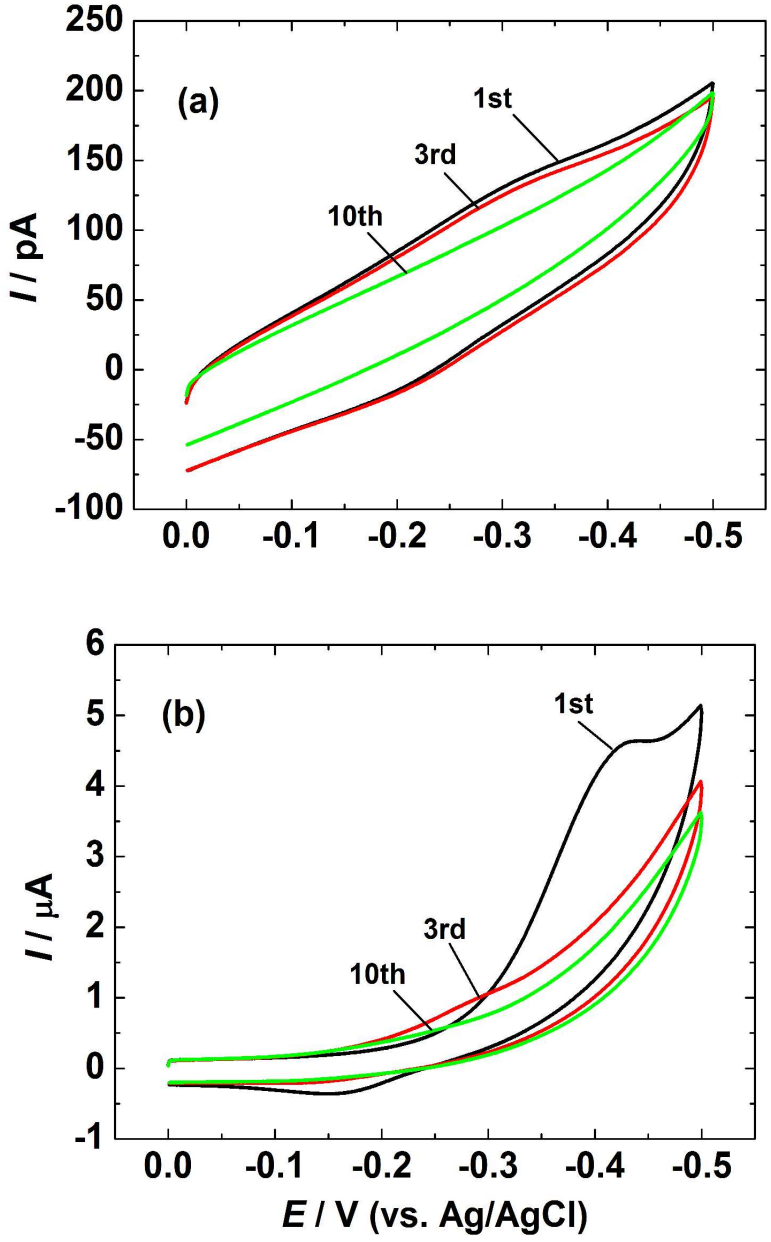


Figure 5.